

# Stratospheric ozone intrusions and impacts on tropospheric ozone

Jesse Greenslade<sup>1</sup>, Simon Alexander<sup>2</sup>, Robyn Schofield<sup>3,4</sup>, Jenny A. Fisher<sup>1,5</sup>, and Andrew Klekociuk<sup>2</sup>

<sup>1</sup>*Center for Atmospheric Chemistry, School of Chemistry,  
University of Wollongong*

<sup>2</sup>*Australian Antarctic Division, Hobart*

<sup>3</sup>*School of Earth Sciences, University of Melbourne*

<sup>4</sup>*ARC Centre of Excellence for Climate System Science, University  
of New South Wales*

<sup>5</sup>*School of Earth & Environmental Sciences, University of  
Wollongong*

September 22, 2016

## Abstract

We develop a quantitative method to identify Stratosphere to Troposphere Transport events (STTs) from ozonesonde profiles. Using this method we estimate the quantity of ozone transported across the tropopause over Melbourne (38°S), Macquarie Island (54°S), and Davis (69°S). STT seasonality is determined from a 7–9 year long time series of ozone profiles from each site. STT events primarily occur during summer above Melbourne and Macquarie Island, while there is little seasonal cycle in STT events above Davis. The majority of tropospheric ozone due to STT events occur within 3 km below the tropopause at Melbourne and Macquarie Island, and within 2 km below the tropopause at Davis. Overall, the fraction of total tropospheric ozone attributed to STT events is 2 – 4% at each site, however, during individual events, an STT event can contribute more than 10% of the total tropospheric ozone at that time. We use the GEOS-Chem model to understand our point-source ozonesonde results in a 3-dimensional context. The GEOS-Chem model run with active stratospheric chemistry is too coarsely resolved in the vertical dimension to determine STTs. Simulated seasonal cycles of tropospheric ozone are well matched at all three sites although vertical profile averages have some bias in the troposphere compared with ozonesondes. A conservative estimate of yearly tropospheric ozone flux due to STTs is calculated using the simulated tropospheric ozone column between 35°S and 75°S of  $2.2 \times 10^{16}$  molecules  $\text{cm}^{-2} \text{yr}^{-1}$  (TODO: update number once model finishes).

# 1 Introduction

Tropospheric ozone constitutes only 10% of the total ozone column but is an important oxidant and greenhouse gas and is toxic to life, harming natural ecosystems and reducing agricultural productivity.. Over the industrial period, increasing tropospheric ozone has been estimated to exert a radiative forcing equivalent to a quarter of the CO<sub>2</sub> forcing [Forster et al., 2007]. Further tropospheric ozone enhancements above pre-industrial levels are projected to drive reductions in global crop yields equivalent to losses of up to \$USD<sub>2000</sub> 35 billion per year (simulated until 2030) [Avnery et al., 2013] along with detrimental health outcomes equivalent to ~11.8 billion per year by 2050 [Selin et al., 2009]. Tropospheric ozone is produced photochemically NO<sub>x</sub> and volatile organic compound emissions, which have both anthropogenic (fossil fuel, biomass combustion) and natural (wildfires, lightning, biogenic) sources. In the upper troposphere, downward transport from the ozone-rich stratosphere provides an additional natural source of tropospheric ozone (Jacobson and Hansson [2000] and references therein).

Stratosphere-to-troposphere transport (STT) primarily impacts the ozone budget in the upper troposphere but can also increase regional surface ozone levels above the legal thresholds set by air quality standards [Danielsen, 1968, Lefohn et al., 2011, Langford et al., 2012, Zhang et al., 2014]. A review of two photochemical models by Stohl et al. [2003] concluded that between 25-50% of tropospheric ozone column can be attributed to SST events, although this mostly affects the upper troposphere. A lower estimate was derived from the Atmospheric Chemistry and Climate Model Intercomparison Project (ACCMIP), Stevenson et al. [2006] found STT was responsible for only ~ 10% (equivalent to  $550 \pm 170$  Tg/yr), with the remainder produced photochemically. The wide range in model estimates exists in part because models are challenged to correctly represent STT. Observation-based process studies are therefore key in determining the relative frequency of SST to the troposphere, with models then able to use this to quantify STT impact over large regions.

STT events are due to deep overshooting convection [Frey et al., 2015], tropical cyclones [Das et al., 2016] and mid-latitude synoptic scale disturbances (e.g. Stohl et al. [2003], Mihalikova et al. [2012]). STT events are strongly dependent on both season and location, for instance over the Mediterranean region, a 10% contribution to tropospheric ozone is estimated between 2000 and 2003 [Galani, 2003], with Lefohn et al. [2011] noting strong seasonal dependence. Notably, STTs have been shown to contribute up to 30% of the surface ozone over the Western US in spring [Lin et al., 2012].

To date, while the frequency, seasonality, and impacts of STT events have been well characterised in the tropics and Northern Hemisphere (NH), observational estimates from the Southern Hemisphere (SH) extra-tropics are noticeably absent from the literature. Since 1998 NASA has tried to standardise ozonesonde release procedures and improve measurement frequency in the SH through the Southern Hemisphere ADDitional OZonesonde (SHADOZ) website (<http://croc.gsfc.nasa.gov/shadoz/>). The papers which have focused on

tropospheric ozone in the SH also note the difficulties that arise from sparse datasets, as many of the sonde releases only occur every two to four weeks and far fewer release sites exist compared to the NH [Liu et al., 2015, Thompson et al., 2014, Mze et al., 2010]. This is further complicated due to ozone intrusion events sometimes lasting for just a matter of hours [Tang and Prather, 2012]. Recently ozonesondes were analysed showing upper tropospheric ozone is increasing near southern Africa, with the increase most likely due to stratospheric mixing [Liu et al., 2015, Thompson et al., 2014]. The extra-tropics in the SH have even less observational studies published.

In the extra-tropics, ozone has a longer photochemical lifetime (TODO: how long?) and STT events most commonly occur during synoptic-scale tropopause folds [Sprenger et al., 2003, Tang and Prather, 2012], and are characterised by tongues of high potential vorticity (PV) air descending to low altitudes. As these tongues become elongated, filaments disperse away from the tongue and mix irreversibly into the troposphere. To date, STT events have been observed in tropopause folds around both the polar front jet [Vaughan et al., 1993, Beekmann et al., 1997], and the subtropical jet [Baray et al., 2000]. They are also observed near cut-off lows [Price and Vaughan, 1993, Wirth, 1995], some of the stratospheric mixing may be due to the turbulent weather which often accompanies these cut-offs. A high correlation has been found between lower stratospheric and tropospheric ozone concentrations [Terao et al., 2008], suggesting mixing between these two layers, with jet streams over the ocean being the major source of transport between the layers.

Ozonesondes are useful for looking at specific locations with high resolution, and in this work they provide an estimate of both STT occurrence rates and STT ozone flux. At these discrete locations, this information can be used in conjunction with regional-scale information in order to estimate large-scale impacts of STT on tropospheric ozone. Here, the GEOS-Chem chemical transport model (CTM) is used to provide the regional-scale ozone concentrations.

Here, we use nearly a decade of ozonesonde observations from three locations spanning latitudes from 38°S - 69°S to characterise the seasonal cycle of STT events and quantify their contribution to the tropospheric ozone budget. In Section 2 we describe the observations and the methods used to identify STT. In Section 3 we examine two case studies to relate STT occurrence to meteorological events. Section 4 provides our newly derived climatologies of STT frequency, seasonality, intrusion altitude, and depth. Section 5 uses these new climatologies to evaluate tropospheric ozone in a global chemical transport model (GEOS-Chem). Finally, we use the observations and the model to estimate the overall contribution of STT events to total tropospheric ozone in the high southern latitudes.

## 2 Data and Methods

### 2.1 Ozone sonde record in the Southern Ocean

Ozone sondes provide a high vertical resolution profile of ozone, temperature, pressure, and humidity from the surface to 35 km.

Ozone mixing ratio is quantified with an electrochemical concentration cell that senses the proportional electrical current from reaction of ozone with a solution of potassium iodide. Standardised procedures are followed when constructing, transporting, and releasing the ozone sondes [NOAA]. Ozone sondes are estimated to provide around 2% precision in the stratosphere, which improves at lower altitudes [NOAA], although the ozone sondes have been shown to be accurate to within 5% as long as the correct procedures are followed [Smit et al., 2007].

Ozone sondes are launched approximately weekly from Melbourne (38°S, 145°E), Macquarie Island (55°S, 159°E) and Davis (69°S, 78°E). For this study, we use the data collected from 2004-2013 for Melbourne and Macquarie, and 2006-2013 for Davis. This is because at these dates we have both ozone and geopotential height (GPH) profiles from the ozone sondes at these sites. At Davis, ozone sondes are launched twice as frequently in the months just prior to and during the ozone hole season (June-October) as at other times of the year [Alexander et al., 2013].

Stratospheric ozone typically mixes irreversibly (vertically and horizontally) into the troposphere in kilometre-scale tongues of air [Frey et al., 2015]. The strength (ozone enhancement above background levels), horizontal scale, vertical depth, and longevity of these intruding ozone tongues vary with weather, topography, and season. This makes the vertical ozone profile recorded by the ozone sonde highly dependent on the time of launch [Sprenger et al., 2003], and it cannot be guaranteed that detected ozone enhancements are fully separated from the stratosphere.

Characterisation of STT events requires a clear definition of the tropopause. The two most common tropopause height definitions are the standard lapse rate tropopause [WMO, 1957] and the ozone tropopause [Bethan et al., 1996]. The lapse rate tropopause is defined as the lowest altitude where the lapse rate (gradient of temperature with altitude) is less than  $2^{\circ} \text{ C km}^{-1}$ , provided the lapse rate between this altitude and all subsequent altitudes within 2 km is also below  $2^{\circ} \text{ C km}^{-1}$ . The ozone tropopause is defined as the lowest altitude satisfying the following three conditions for the ozone mixing ratio (OMR) [Bethan et al., 1996]:

1. Vertical gradient of OMR is greater than  $60 \text{ ppbv km}^{-1}$
2. OMR is greater than 80 ppbv
3. OMR exceeds 110 ppbv between 500 m and 2000 m above the altitude under inspection (500 m and 1500 m in the Antarctic, including the site at Davis).

The ozone tropopause can be less robust during stratosphere-troposphere exchange, however it is more robust than the lapse rate tropopause at polar latitudes in winter and near jet streams in the lower stratosphere due to temperature inversions near the tropopause definition region [Bethan et al., 1996, Tomikawa et al., 2009, Alexander et al., 2013]. In this work the lower of these two tropopause altitudes is used, as both are calculated for each ozonesonde release. Here, we calculate both tropopause heights for each ozonesonde release and use whichever is lower. This choice avoids occasional unrealistically high tropopause heights due to perturbed ozone or temperature measurements in the ozonesonde data.

Figure 1 shows the monthly mean tropopause altitudes at each location (solid lines). The dashed lines in Figure 1 show the mean tropopause altitude calculated from the subset of ozonesondes that detected an STT event. The seasonal cycle in tropopause altitude at Melbourne is exhibited, showing a maximum in summer, and a minimum in winter. This cycle is much more subtle at Macquarie, and almost reversed at Davis, which has a minimum during autumn and maximum from winter to spring. The decreasing tropopause altitude which occurs at higher southern latitudes is also apparent, as lower mean tropopause heights occur with more southern latitudes. The tropopause is higher on days with an STT event at all during winter and spring at Davis.

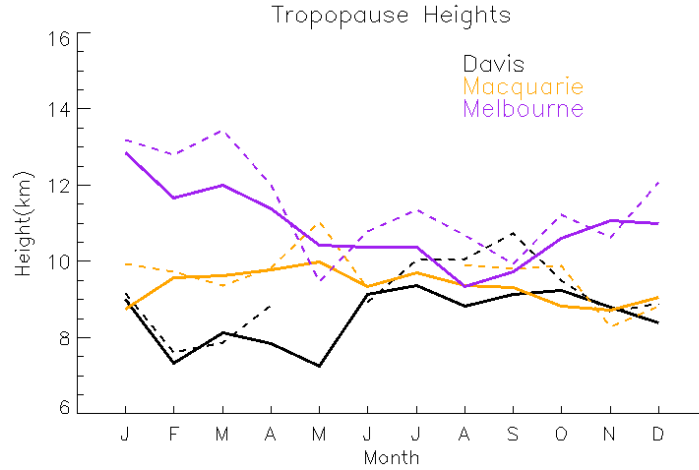


Figure 1: Multi-year monthly mean tropopause altitude (minimum of lapse rate and ozone defined tropopause) determined from ozonesondes measurements at Melbourne (2004-2013), Macquarie (2004-2013) and Davis (2006-2013) (solid lines). Dashed lines show the monthly mean tropopause altitude for the subset of dates when STT events occurred. (TODO: vertical shaded 90th percentiles, change height label to altitude)

Figure 2 shows multi-year averaged ozone mixing ratios measured by ozonesonde

over the three stations. Over Melbourne, increased ozone extending down through the troposphere is apparent from December to March and September to November. The increased tropospheric ozone in these months are due to STTs (in summer), and possible fire smoke plume influence (in winter), discussed in more detail below. Over Davis and Macquarie Island, the tropospheric ozone is higher between March and October, although the seasonal differences are small compared to those at Melbourne. This seasonality at the high latitude sites is driven by a decrease in photochemical destruction when the solar zenith angle is greater, causing light to have longer path length and reduced radiation (TODO: read and cite S. Oltmans antarctic papers - re Andrews comment).

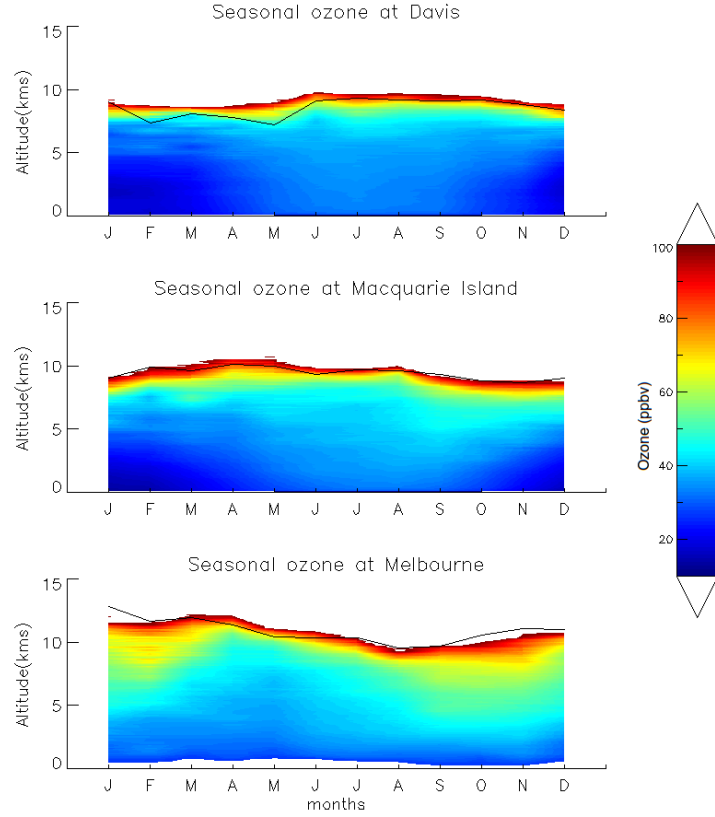


Figure 2: Multi-year mean seasonal cycle of ozone mixing ratio over Davis, Macquarie, and Melbourne measured by ozonesondes. Measurements were binned monthly and interpolated between months. Black solid lines show mean tropopause altitudes, defined as described in the text.

## 2.2 Model description

GEOS-Chem is a global chemical transport model [Bey et al., 2001], which includes transport, emission, deposition, chemical production and destruction of ozone and 103 other trace gases throughout the troposphere along with stratospheric chemistry, including photolysis. Stratosphere-troposphere coupling is calculated using the stratospheric unified chemistry extension (UCX) [Eastham et al., 2014], which includes a further 28 trace gases. For comparison to ozonesonde observations, we use GEOS-Chem version 10-011 (including UCX) run from 2005-2012, following a 1-year spin-up for 2004. Transport is driven by assimilated meteorological fields from the Goddard Earth Observing System (GEOS-5) maintained by the Global Modeling and Assimilation Office (GMAO) at NASA. Biogenic emissions of organic chemicals are determined by the Model of Emissions of Gases and Aerosols from Nature (MEGAN) version 2.1 extended by Guenther et al [Guenther et al., 2012]. Anthropogenic emissions are given by the Emissions Database for Global Atmospheric Research (EDGAR) version 4.2.

Our simulation was modified from the standard v10-01 to a fix a bug in the treatment of the Total Ozone Mapping Spectrometer (TOMS) satellite data used to calculate photolysis (see Henderson [2016]). The simulation uses  $2^\circ$  latitude by  $2.5^\circ$  longitude horizontal resolution, with 72 vertical levels from the surface to 0.1 hPa. For the three sites, a vertical profile of ozone is stored every 6 hours, based on standard UTC+0 time. This means that the GEOS-Chem profiles which match ozonesonde release hours are local times of 7AM, 11AM, and 11AM for Davis, Macquarie, and Melbourne respectively.

## 2.3 Characterisation of STT events and associated fluxes

We characterise STT events using the ozonesonde vertical profiles to identify tropospheric ozone volume mixing ratio enhancements above a local background (in moles per billion moles of dry air, or ppb). Calculation of ozone transport is performed after converting the profile to molecules  $\text{cm}^{-3}$ . The process is illustrated in Figure 3 for an example ozone profile.

First, the ozone vertical profiles are linearly interpolated to a regular grid with 20 m resolution from the surface to 14 km altitude. The interpolated profiles are then bandpass filtered using a Fourier transform to retain perturbations with vertical scales between 0.5 km and 5 km (removing low and high frequency perturbations). In what follows, these filtered vertical profiles are referred to as perturbation profiles. The choice of band limits was set empirically. For an event to qualify as STT, a clear increase above the background ozone level is needed, and we find that a vertical limit of  $\sim 5$  km removes seasonal-scale effects. The 0.5 km scale limit is set in order to remove any spikes of ozone which could be considered noise. We next use all the perturbation profiles at each site to calculate the 99th percentile perturbation value for the site. This is considered our threshold for tropospheric ozone perturbations, and perturbations above this threshold in individual ozonesondes are classified as STT events.

## Ozone at Melbourne on 2004/01/08

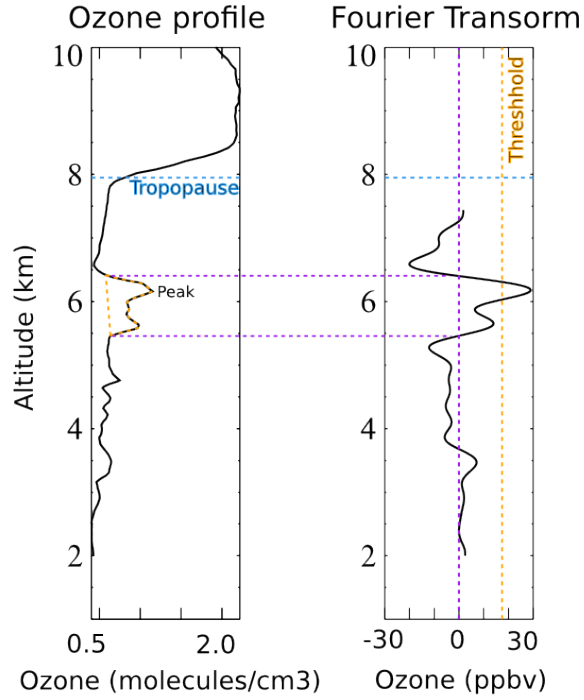


Figure 3: An example of the STT identification and flux estimation methods used in this work. The left panel shows an ozone mixing ratio profile from Melbourne on the 8th of January 2004 from 2km to the tropopause (dashed horizontal line). The right panel shows the perturbation profile created from bandpass filtering of the mixing ratio profile. The STT occurrence threshold calculated from the 99th percentile of filtered ozone perturbations is shown with the orange dashed line, and the technique for determining the vertical extent of the event is shown with the purple dashed lines (see details in text). The ozone flux associated with the STT event is calculated using the area outlined with the orange dashed line in the left panel.



STTs which occur at altitudes below 4 km are removed in order to avoid surface pollution events. Those occurring within 0.5 km of the tropopause are also removed in order to avoid spurious false positives induced by the sharp transition to stratospheric air.

Finally, we define the ozone peak as the altitude where the OMR is greatest within the lowest range of altitudes where the perturbation profile exceeds the percentile-based threshold. If the perturbation profile drops below zero between the ozone peak and the tropopause, the STT event is confirmed. Alternatively, if the OMR between the ozone peak and the tropopause drops below 80 ppb and is at least 20 ppb lower than the OMR at the ozone peak, the STT event is also confirmed. Otherwise the profile is rejected as a non-event. This final step removes near-tropopause anomalies for which there is no evidence of detachment from the stratosphere.

We estimate the ozone flux into the troposphere associated with each event by integrating the ozone concentration enhancement vertically over the altitude range for which an STT event is identified (i.e. the range surrounding the ozone peak over which the perturbation profile is greater than zero). This estimate is conservative because it does not take into any secondary ozone enhancements that may have been caused by the STT, and also ignores any heightened ozone background levels which may be due to synoptic-scale stratospheric mixing into the troposphere.

Tang and Prather [2010] define one possible method for detecting STT events from ozonesonde measurements. Their definition is based on subjective analysis of sondes released from 20 stations in the latitudinal range from 35°S to 40°N. In their work, a tropopause fold has occurred if, starting from 5 km altitude, the ozone level exceeds 80 ppb and then within 3 km decreases by 20 ppb or more to a value less than 120 ppb.

## 2.4 Biomass burning influenced events

The STT detection algorithm described in Section 2.3 assumes all mid-upper troposphere ozone perturbations above the 99th percentile are caused by stratospheric intrusions. In some cases, however, these perturbations may in fact reflect ozone production in lofted smoke plumes. Biomass burning in southern Africa and South America has previously been shown to have a major influence on atmospheric composition in the vicinity of our measurement sites [Gloude-mans et al., 2007, Edwards et al., 2006], particularly from July to December [Pak et al., 2003]. On occasion, Australian and Indonesian fires can also reach the mid-high southern latitudes, which is seen when examining the carbon monoxide (CO) from the AIRS (Atmospheric Infrared Sounder) instrument on board the Aqua satellite [AIR, 2013].

Large biomass burning events emit substantial quantities of ozone precursors, some of which are capable of being transported long distances and driving ozone production far from the fire source [Jaffe and Wigder, 2012]. Ozone production from biomass burning is complex and affected by photochemistry, fuel nitrogen load, and time since emission. While ozone production occurs in some

biomass burning plumes, this is not always the case; therefore ozone perturbations detected during transported smoke events may or may not be caused by the plume. We therefore flag all detected STT events found near smoke plumes but do not exclude them from our final dataset.

Possible biomass burning influence is identified using satellite observations of CO from the AIRS instrument. CO is emitted during incomplete combustion and is an effective tracer of long-range transport due to its long lifetime. In the Southern Hemisphere, biomass burning is the primary source of CO, making CO a good proxy for fire plumes (eg: Edwards [2003], Sinha et al. [2004], Edwards et al. [2006], Mari et al. [2008]).(TODO: split citations to their most appropriate sentences) We use data from the AIRS (Atmospheric Infrared Sounder) instrument on board the Aqua satellite [AIR, 2013]. To identify possible biomass burning influence, we visually inspected AIRS vertical columns CO in the vicinity of our three measurement sites for all dates with detected STT events. We diagnose smoke plumes as areas with elevated CO columns ( $\sim 2 \times 10^{18}$  molecules  $\text{cm}^{-2}$  or higher), and flag any sonde-detected STT event that occurs near a smoke plume.

Figure 4 contrasts two days with and without signs of biomass burning influence near the Melbourne site (purple circle). 17 October 2007 (top) shows a day where elevated CO suggests the site may have been influenced by long-range transport from African and/or South American biomass burning. In contrast, on 3 February 2006 (bottom) CO columns across the Southern Hemisphere show no influence from biomass burning. We screened all days with detected STT events except one event during which there were no available AIRS data (January 2010), and found that biomass burning may have influenced 21% of events over Melbourne and 17% of events over Macquarie island. These events are flagged in the following sections, and are not used in our calculation of total STT flux. All of the flagged events except for one (in January at Macquarie Island) occur within the Southern Hemisphere burning season (July to December). No events at Davis were influenced by smoke transport.

## 2.5 Sensitivities and limitations

Our method uses several subjectively defined quantities in the process of STT event detection. Here we briefly discuss these and the sensitivity to each. Using the algorithm discussed in section 2.3, we detect 45 events at Davis, 47 (+8 fire influenced) events at Macquarie Island, and 72(+14 fire influenced) events at Melbourne.

The cut-off threshold (defined separately for each site) is determined from the 99th percentile of the ozone perturbations between 2 km and 1 km below the tropopause. We use the 99th percentile because at this point the filter locates clear events with no obvious false positives. Event detection is highly sensitive to this choice; for example, using the 98.5th percentile instead increased detected events by 24 at Melbourne (33%), 19 at Macquarie Island (40%), and 10 at Davis (22%). This high sensitivity means that detection is also sensitive to the profile altitude bounds used in calculation of the percentiles, i.e. the

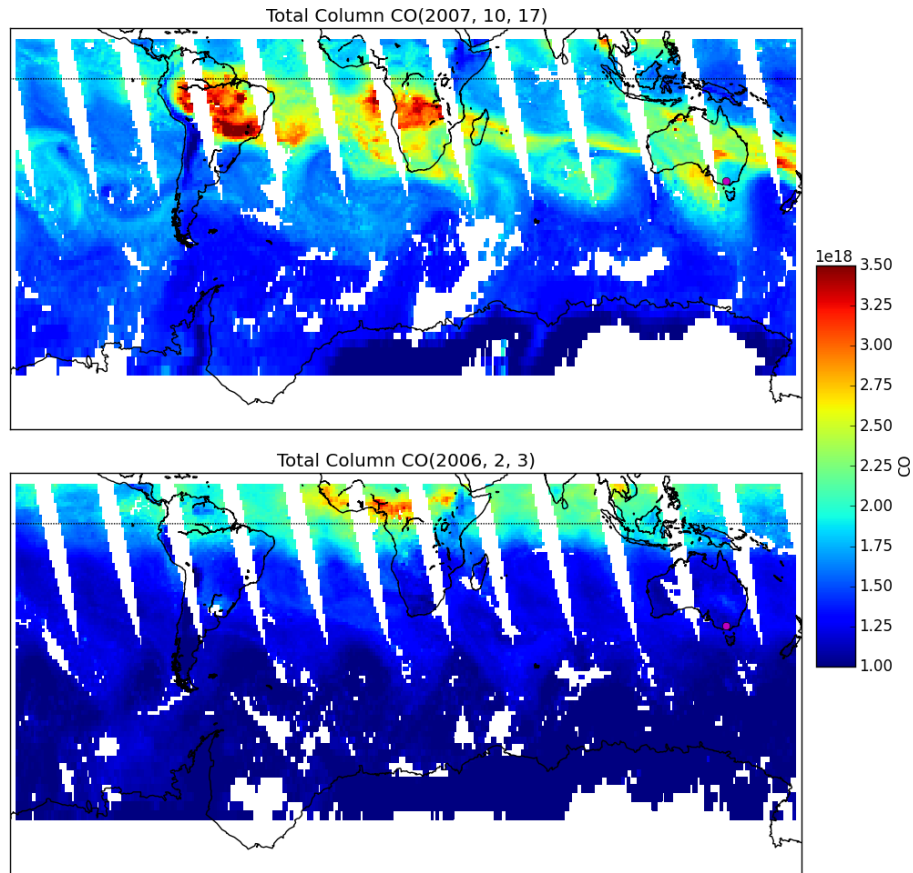


Figure 4: Example detection of biomass burning influence using AIRS total column CO. The top panel (17 October 2007) shows a day when ozone above Melbourne (purple dot) could have been caused by a transported biomass burning plume, and so was flagged in subsequent analysis. The bottom panel (3 February 2006) shows a day when Melbourne ozone was not influenced by transported smoke.

2 km altitude to 1 km below the tropopause range. The altitude range used to determine the 99th percentile is set from 2 km up to 1 km below the tropopause. This range removes any anomalous edge effects of the Fourier bandpass filter, as well as discounting the highly variable ozone concentration which occurs near the tropopause. Finally, ozone enhancements are only considered STT events if they occur above 4 km and within 500 m below the tropopause. This range removes possible ground pollution, as well as allowing event detection up to 500 m from the tropopause. Some events, including the storm-caused event examined in figure 5 are within one kilometer of the tropopause.

The event detection was not as sensitive to the choice of Fourier bandpass scales; A widening of the allowed scales to the range 0.4-5.1 increased the detected events by 3 at Melbourne, 2 at Macquarie Island, and Davis lost two events (there are more detected events, but more being filtered out).

Flux estimation over the southern ocean is based on the average GEOS-Chem tropospheric vertical column of HCHO over a particular latitude range. The range is from 35°S to 75°S, changing this latitude range by 5° in either direction at either end of the range changes the average simulated tropospheric ozone by -8 to 9%.

## 2.6 Classifying synoptic conditions during STT events

An investigation of the ERA-I synoptic weather during STT events above (at 500 hPa) Melbourne, Macquarie Island, and Davis are used to subjectively classify the events based on their likely cause. Typically during STT occurrence, the upper troposphere is not calm, with low pressure fronts or cut-offs nearby at coincident time. Similar characteristics are seen over Melbourne and Macquarie Island: i.e. a prevalence of frontal and low pressure activity during STT events. Over Davis the weather systems are harder to distinguish, and the stratospheric polar vortex may create ozone folds without other sources of upper tropospheric turbulence.

We examine two case studies in detail to illustrate the synoptic-scale conditions in which STT events occur over Melbourne. Data from the European Center for Medium-range Weather Forecasts (ECMWF) Interim Reanalysis (ERA-I) [Dee et al., 2011] product are used for synoptic-scale examination of weather patterns over our three sites on dates matching detected STT events.

Figure 5 (left) shows the ozonesonde profile above Melbourne on 3 of February 2005. The tropopause was between 400 and 500 hPa and ozone in the upper troposphere was anticorrelated with relative humidity, suggesting the ozone enhancements derived from dry stratospheric air. An ozone intrusion into the troposphere at  $\sim 520$  hPa was identified by our detection algorithm. Figure 5(right) shows the concurrent synoptic weather system, a cut-off low pressure system that caused a large storm and lowered the local tropopause height for several days. These systems also increase turbulence near the tropopause, which can lead to increased transport events. The flux of stratospheric ozone into the troposphere associated with this event, calculated using the method shown in section 2.3, was at least  $3.1 \times 10^{11}$  molecules  $\text{cm}^{-3}$ , or 8% of the tropospheric

ozone column.

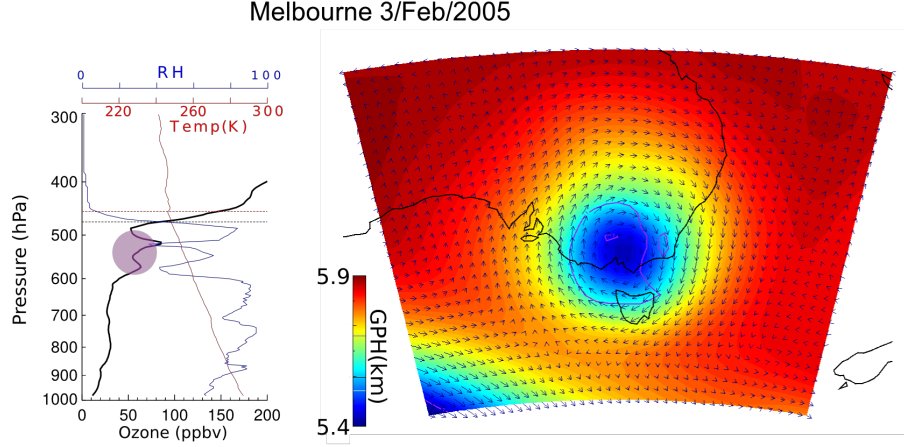


Figure 5: (Left) Vertical profile of ozone (black), relative humidity (blue), and temperature (red) measured by ozonesonde over Melbourne on 3 February 2005. The detected ozone STT event is highlighted in pink. Tropopause heights using both the ozone definition (black dashed line) and lapse rate definition (red dashed line) are also shown. (Right) Geopotential heights at 500 hPa from the ERA-Interim reanalysis, with wind vectors overplotted. Also shown are contours of potential vorticity units with 1 PVU in purple.

Figure 6 (left) shows the vertical ozonesonde profile recorded on the 13th January 2010 over Melbourne. Figure 6 (left) shows the ozonesonde profile over Melbourne on 13 January 2010. The tropopause was higher on this date (120-160 hPa). Using our algorithm, we detected an ozone intrusion centred around 200 hPa. As before, ozone anticorrelation with relative humidity provides further evidence that the elevated ozone was stratospheric in origin. In this profile, there was clear separation between the detected intrusion (highlighted in pink) and the ozone tropopause (black dashed line), which indicates that the sonde passed through regular tropospheric air after hitting a stratospheric intrusion but before reaching the tropopause. Figure 6 (right) shows that this event was associated with a trough of low pressure (front) passing over southeastern Australia. This front traveled from west to east and caused a wave of lowered tropopause height. Frontal passage is a known cause of STT as stratospheric air descends and streamers of ozone-rich air break off and mix into the troposphere [Sprenger et al., 2003].

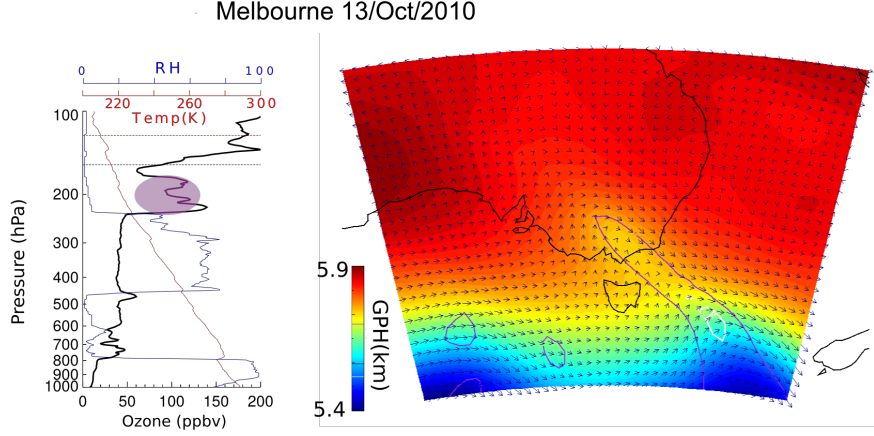


Figure 6: Same as Figure 5 but for 13 January 2010. Also shown in this figure is the 2 PVU contour (white), often used to determine dynamical tropopause height.

### 3 STT event climatologies

re 7 shows the seasonal cycles of STT events detected at Melbourne, Macquarie Island, and Davis. STT events in Figures 7-9 are coloured based on the meteorological classification described in Section 2.6, with events classified as either low pressure fronts (“frontal”, dark blue), cut-off low pressure systems (“cutoff”, teal), or indeterminate (“misc”, cyan). Events that may have been influenced by transported smoke plumes (Section 2.4) are shown in red. (TODO: Event count, including types)

There is an annual cycle in the frequency of STT events (Fig. 7) with a summertime peak above Melbourne and Macquarie Island. This summertime peak is due to an increased prevalence of summer low-pressure storms and fronts, which increase turbulence and lower the tropopause [Reutter et al., 2015]. For both Melbourne and Macquarie Island, the STT events which are unlikely to be fire-related occur mostly in summer during these low pressure synoptic systems.

At Davis, the frequency of STT events is relatively constant throughout the year, with a slight increase during Antarctic winter. STT events associated with cut-off low pressure systems are more prevalent during winter, while STT events associated with frontal passage occur throughout the year. The polar vortex and associated lowered tropopause may be partially responsible for the STTs detected in winter. We were unable to meteorologically classify most summertime events at Davis.

The slightly increased winter time frequency of STT events at Davis may be

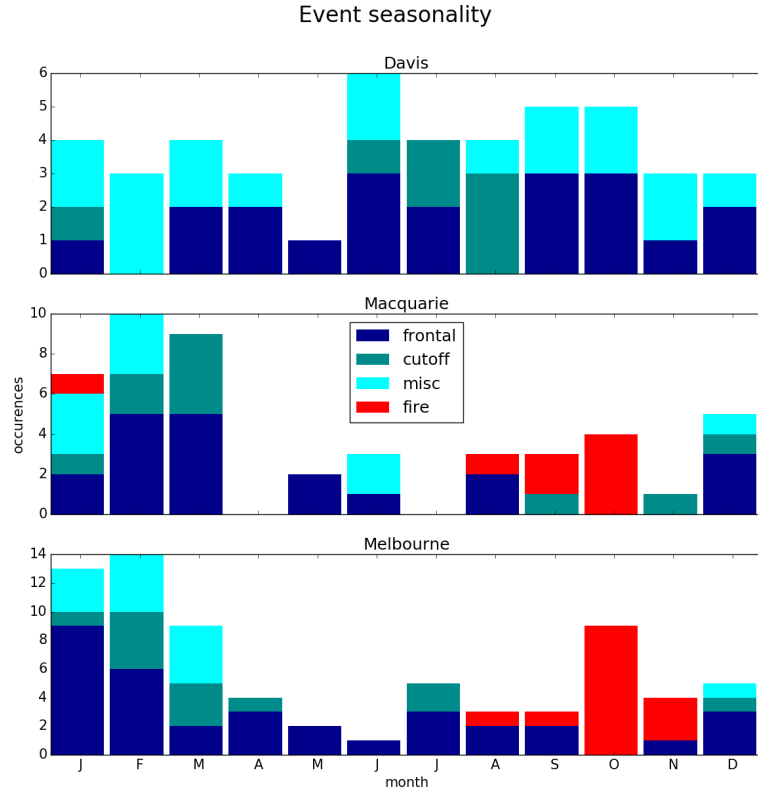


Figure 7: Seasonal cycle of STT events detected at Davis (top), Macquarie Island (middle), and Melbourne (bottom). Events are categorised by associated meteorological conditions as described in the text, with low pressure fronts (“frontal”) in dark blue, cut-off low pressure systems (“cutoff”) in teal, and indeterminate meteorology (“misc”) in cyan. Events that may have been influenced by transported smoke plumes are shown in red (see text for details).

attributable to the increased frequency of sonde releases from June to October (see Section 2.1). It is also possible that the sample of only 45 detected events over 10 years is too small to detect any seasonality.

Figure 8 shows the altitudes of detected events, based on the altitude of peak (maximum) tropospheric ozone in the ozonesonde profile. STT event peaks most commonly occur at 6 – 10 km above Melbourne and 6 – 9 km at Davis but are distributed more evenly at Macquarie Island from 4 – 7.5 kilometres altitude. There is no clear relationship between meteorological conditions and event altitude.

Figure 9 shows the distance from the tropopause of the peaks of detected events, based on the distance between the peak ozone peak associated with the detected STT event and the tropopause (using the lowest of the two tropopause definitions), as described in Section 2.1. The majority of STT events occur within 3 km of the tropopause at both Melbourne and Macquarie Island, and within 2 km of the tropopause at Davis. Again, there is no clear relationships between meteorological conditions and event depth.

## 4 Comparison with GEOS-Chem

Figure 10 compares the time series of tropospheric ozone column ( $\Omega_{O_3}$ ) in molecules  $\text{cm}^{-2}$  simulated by GEOS-Chem (red dots) to the measured tropospheric ozone columns (black stars). Sonde tropospheric columns are calculated using the GPH and ozone partial pressure recorded by the ozonesondes, using (TODO: equation here.) The seasonal cycles are well correlated, with similar timing and magnitude (paired  $r^2$  values of TODO: run script when model run finished). In both observations and model, the maximum ozone column at Melbourne occurs in summer, with a minimum in winter, while Macquarie and Davis show the opposite seasonality. The model shows more day-to-day variability than the ozonesondes, although there are daily simulated values for the model while only weekly or less for the ozonesondes. (TODO: Verify this)

Figure 11 shows the observed and simulated ozone profiles at all sites, averaged seasonally. The model generally underestimates ozone at low altitudes (up to 6 km) at both Davis and Macquarie, although this bias is less pronounced during summer. Over Melbourne, ozone in the lower troposphere is well represented, but the model overestimates ozone from around 4 km to the tropopause. Also notable is the lower tropopause height simulated by the model, which on average is  $\sim 1$  km lower than observed (TODO: mean bias, updated when model finishes). The effect of local pollution can be seen over Melbourne, mostly during the austral summer months (DJF), as the increased mean mixing ratios and enhanced variance near the surface.

TODO: up to here with Jenny Comments

Although GEOS-Chem reasonably matches the ozonesonde tropospheric ozone column, it does not have the resolution required to capture STTs. Figure 12 shows the best (left) and worst (right) comparisons of ozone profiles up to 14 km between the ozonesondes and GEOS-Chem. The model output is shown in red,



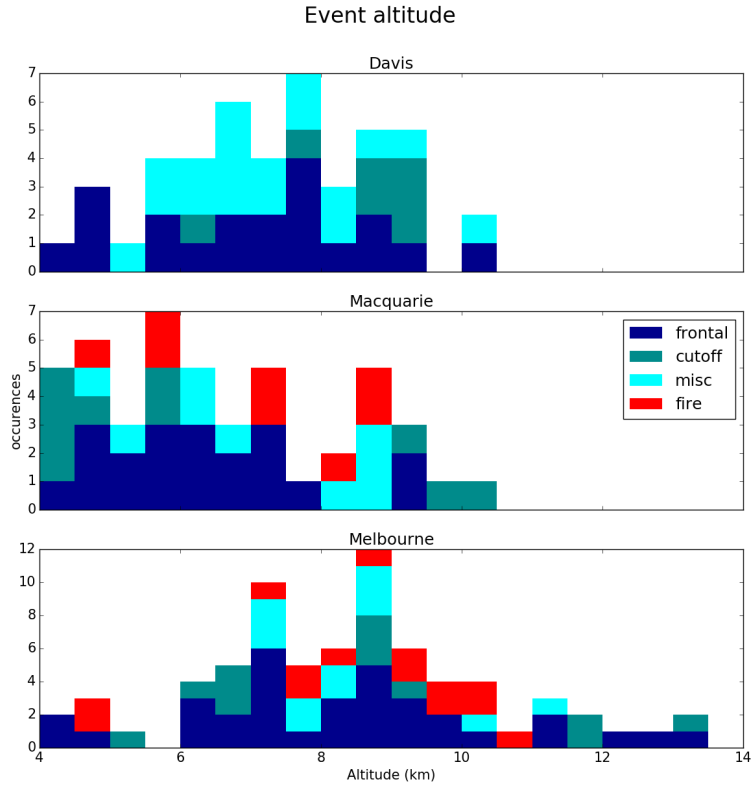


Figure 8: The distribution of STT event altitude at Davis (top), Macquarie Island (middle), and Melbourne (bottom), determined as described in the text. Events are coloured as described in Fig. 7.

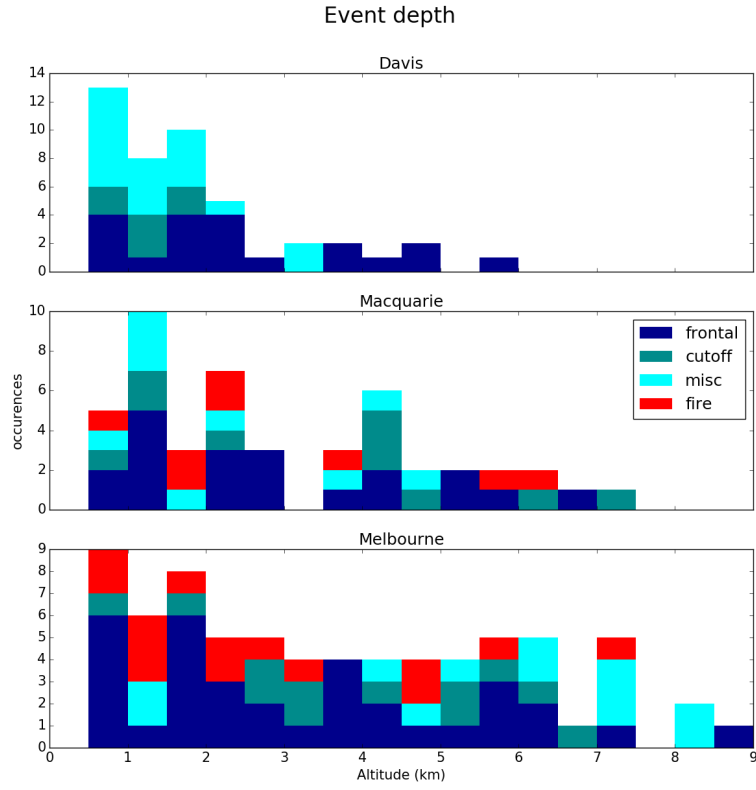


Figure 9: The distribution of STT event distance from the tropopause at Davis (top), Macquarie Island (middle), and Melbourne (bottom), determined as described in the text. Events are coloured as described in Fig. 7.

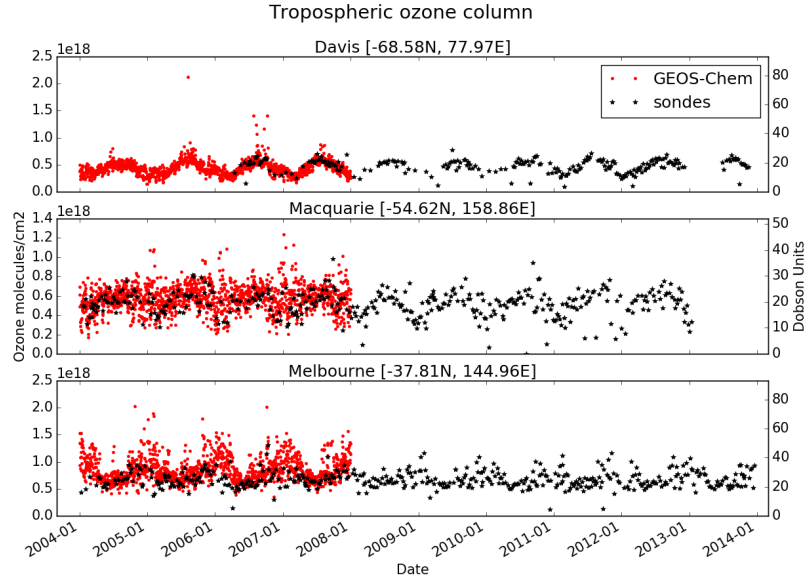


Figure 10: Tropospheric ozone column ( $\Omega_{O_3}$ , in molecules  $\text{cm}^{-2}$ ) at daily resolution simulated by GEOS-Chem (grey dots) from January 1 2004 to April 31 2013. Simulated points which are on the same day as an ozonesonde are displayed in red. For each plot, the model has been sampled in the grid square containing the site. Columns calculated from ozonesondes are shown as black stars, each representing one measurement. (TODO: Update once fixed model run finishes)

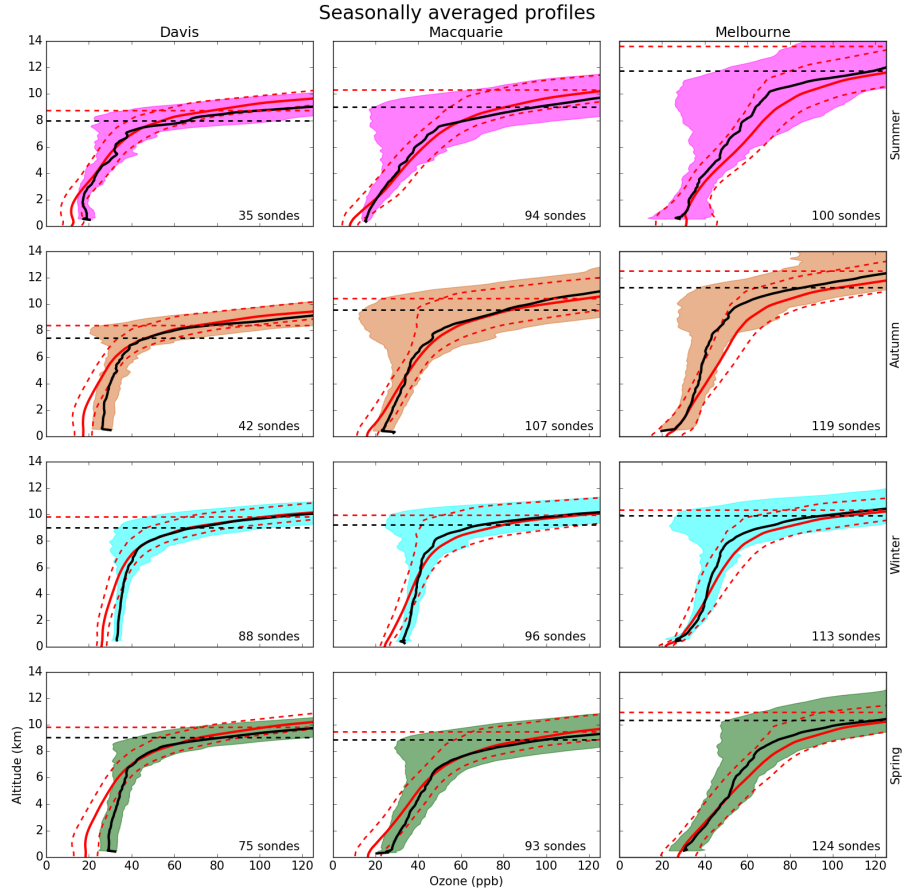


Figure 11: Observed and simulated tropospheric ozone profiles over Davis, Macquarie, and Melbourne, averaged seasonally. Model means (2005-2013 average) is shown as red solid lines, with red dashed lines showing the 10th and 90th percentile. Ozonesonde means (over each season, for all years) are shown as black solid lines, with coloured shaded areas showing the 10th and 90th percentile. The horizontal dotted line shows the mean tropopause heights from the model (red) and the observations (black). TODO: Update once fixed model run finishes.

and is the average over  $2^\circ$  latitude by  $2.5^\circ$  longitude which contain the respective sonde release site. The vertical resolution from GEOS-Chem is too low to allow detection of STTs, with roughly 30 vertical levels up to the tropopause, while sondes have upwards of 100.

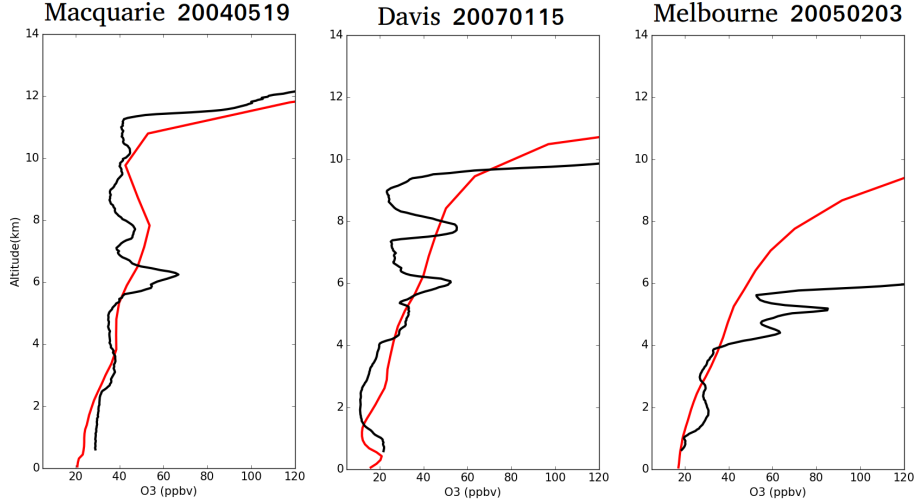


Figure 12: Ozonesonde profiles (black) against GEOS-Chem profiles (red) for three different dates, one over each site. The dates were picked based on subjective visual analysis as follows: left is the best match - May 19th 2004 over Macquarie, middle is an average case - January 15th, 2007 over Davis, and right is the worst match - February 3rd 2005 over Melbourne.

## 5 Stratosphere to troposphere ozone flux from STT events

Based on the integrated ozone amount associated with each STT event (see section 2.3), we find a lower bound for the STT ozone flux over each of our three sites (fire influence excluded). This is a conservative lower bound as the algorithm ignores secondary ozone peaks which may also be transported down from the stratosphere, as well as ignoring potential ozone dispersion from the ozone peak. Figure 13 shows the mean fraction of total tropospheric column ozone attributed to stratospheric ozone intrusions at each site, averaged over days when an STT event occurs. The mean fraction of tropospheric ozone attributed to STT events is 2–4%, on individual days this value can exceed 10% at Macquarie and Melbourne. Figure 14 shows the data in absolute terms, and indicates that the mean STT event impact is around  $1$  to  $2 \times 10^{16}$  molecules/cm<sup>2</sup>. Our flux estimates are relatively insensitive to our biomass burning filter; including

smoke-influenced days changes the mean flux by less than 0.25% (5% relative change).

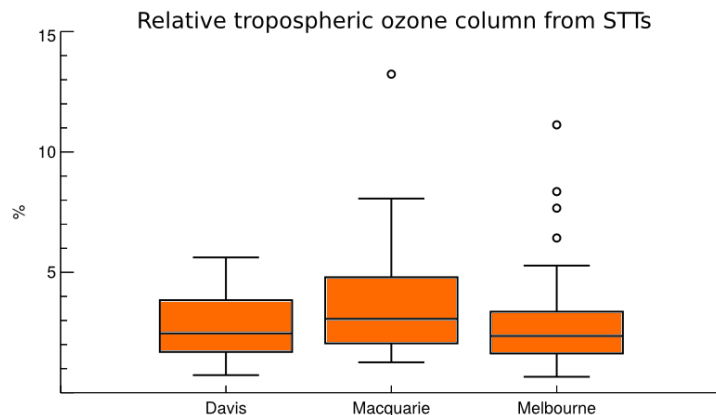


Figure 13: Fraction of total tropospheric column ozone attributed to stratospheric air intrusions during STT events.

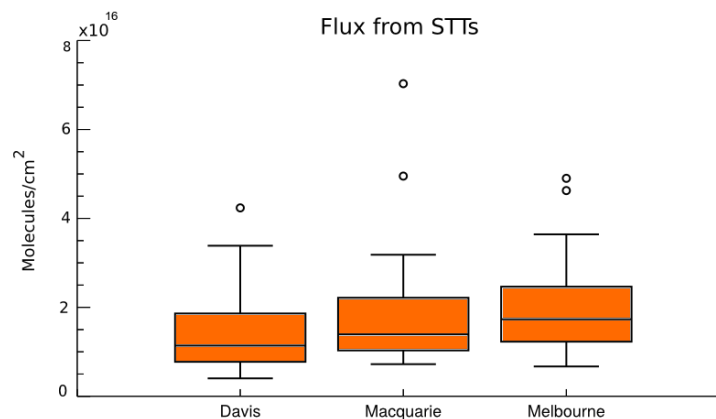


Figure 14: Tropospheric ozone attributed to stratospheric air intrusions during STT events.

Extrapolating out over the Southern Ocean using our estimated enhanced tropospheric ozone, we can create a rough estimate of the STT effect on tropospheric ozone in this region. This is be done by multiplying the monthly likelihoods of STTs with the monthly tropospheric column ozone amounts multiplied by our mean flux fraction. Taking the monthly likelihood from our ozonesonde

events count per sondes released during each month, and southern latitude tropospheric column ozone amount from GEOS-Chem, the total amount of ozone from STT events over the southern ocean is at least (TODO:update once fixed model is finished)  $2.2 \times 10^{16}$  molecules  $\text{cm}^{-2} \text{yr}^{-1}$ , TODO: this is around X:TG/yr ozone. Figure 15 shows the seasonal STT contribution calculated this way, with ‘l’ and ‘f’ being the STT likelihood and fraction respectively.

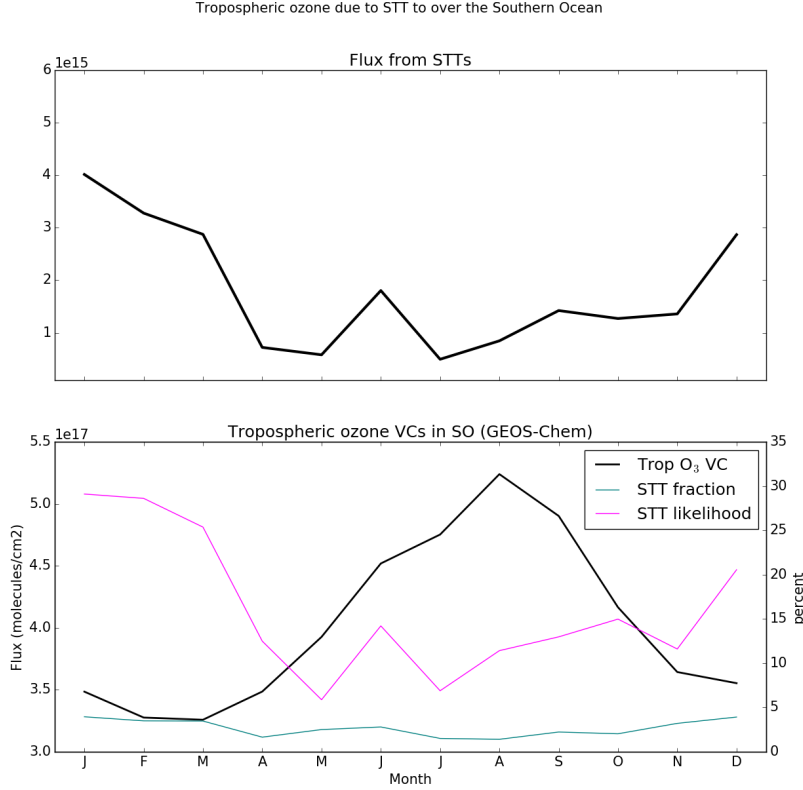


Figure 15: Top panel shows the estimated STT contribution to tropospheric ozone VC. Bottom panel shows the three factors multiplied together in order to produce the estimation. Units for ‘l’ and ‘f’ are on the right, while units for ozone VC amounts are on the left.

Our estimate is ( todo: greater/smaller/completely different) to other estimates of southern hemispheric ozone transport. Olsen [2003] use PV and winds from GEOS along with ozone measurements from TOMS to estimate that around 210 TG  $\text{yr}^{-1}$  of ozone flux occurs in 2000 between 30°S and 60°S. Their estimates show a peak in flux from winter to early spring (JJAS), which is the same months when our GEOS-Chem simulation shows the highest tro-

pospheric  $\Omega_{O_3}$ . Global STT flux estimated from an ensemble of models shows global STT flux at around  $550 \text{ Tg yr}^{-1}$  [Stevenson et al., 2006]. Global net flux (transport from the stratosphere to the troposphere minus opposite transport) is estimated to be  $75 \text{ Tg yr}^{-1}$  [Sprenger et al., 2003].

Considering the individual event contributions, Terao et al. [2008] estimate much higher STT impacts; where 30–40% of the tropospheric column is due to STT. Although this figure is based on the Northern Hemisphere during the seasonal STT peak.

## 6 Conclusions

Ozonesonde data in the Southern Hemisphere provides a satellite-independant quantification of STT ozone transport. The frequency and amount of ozone descending from the stratosphere into the troposphere can be estimated from the long time series of tropospheric ozone profiles. Using almost ten years of ozonesonde profiles over the southern high latitudes, a clear summer peak is seen for STT occurrences at both  $38^\circ\text{S}$  and  $55^\circ\text{S}$ , although not at  $69^\circ\text{S}$ .

We use a Fourier bandpass filter to determine STT ozone transport events. The filter removes seasonal tropospheric ozone influences and allows clear detection of ozone-enhanced tongues of air in the troposphere. By setting empirical checks, ozonesonde vertical profiles can clearly show tropospheric ozone enhancement which is separated from the stratosphere. The cause of these ozone enhancements is examined through the use of satellite and reanalysis datasets on case studies above Melbourne. The major causes of STT events found over Melbourne are turbulent weather in the upper troposphere due to low pressure fronts and cut-off low pressure systems. TODO: Discuss Davis, Macq here

Integration of the ozone enhancement along the altitude of the ozone profile allows a rough estimate of stratospheric transport for each event. Events typically cause a 3% enhancement of the tropospheric ozone column. This is around  $2 \times 10^{15} \text{ molecules cm}^{-2}$  (TODO: Update when model run finishes) ozone enhancement over the southern high latitudes caused by STTs.

GEOS-Chem performs fairly well when compared to ozonesondes at our three sites, with vertical profile averages and seasonal cycles of tropospheric ozone conforming to within  $\sim 10\%$  (TODO: update when model finishes) of the data, even though the model is looking at the average over  $2^\circ$  latitude by  $2.5^\circ$  longitude grid boxes.

## References

AIRS3STD, 2013.

S. P. Alexander, D. J. Murphy, and A. R. Klekociuk. High resolution VHF radar measurements of tropopause structure and variability at Davis, Antarctica ( $69^\circ\text{S}$ ,  $78^\circ\text{E}$ ). *Atmospheric Chemistry and Physics*, 13(6):3121–3132,



2013. ISSN 16807324. doi: 10.5194/acp-13-3121-2013. URL <http://www.atmos-chem-phys.net/13/3121/2013/>.
- Shiri Avnery, Denise L. Mauzerall, Junfeng Liu, and Larry W. Horowitz. Global crop yield reductions due to surface ozone exposure: 2. Year 2030 potential crop production losses and economic damage under two scenarios of O<sub>3</sub> pollution. *Atmospheric Environment*, 71(13):408–409, 2013. ISSN 13522310. doi: 10.1016/j.atmosenv.2012.12.045. URL <http://dx.doi.org/10.1016/j.atmosenv.2011.01.002>.
- J. L. Baray, V. Daniel, G. Ancellet, and B. Legras. Planetary-scale tropopause folds in the southern subtropics. *Geophysical Research Letters*, 27(3):353–356, 2000. ISSN 00948276. doi: 10.1029/1999GL010788.
- M. Beekmann, G. Ancellet, S. Blonsky, D. De Muer, A. Ebel, H. Elbern, J. Hendricks, J. Kowol, C. Mancier, R. Sladkovic, H. G J Smit, P. Speth, T. Trickl, and Ph Van Haver. Regional and global tropopause fold occurrence and related ozone flux across the tropopause. *Journal of Atmospheric Chemistry*, 28(1-3):29–44, 1997. ISSN 01677764. doi: 10.1023/A:1005897314623.
- S. Bethan, G. Vaughan, and S. J. Reid. A comparison of ozone and thermal tropopause heights and the impact of tropopause definition on quantifying the ozone content of the troposphere. *Quarterly Journal of the Royal Meteorological Society*, 122(532):929–944, 1996. ISSN 00359009. doi: 10.1002/qj.49712253207. URL <http://doi.wiley.com/10.1002/qj.49712253207>.
- Isabelle Bey, Daniel J. Jacob, Robert M. Yantosca, Jennifer A. Logan, Brendan D. Field, Arlene M. Fiore, Qin-Bin Li, Hong-Yu Liu, Loretta J. Mickley, and Martin G. Schultz. Global Modeling of Tropospheric Chemistry with Assimilated Meteorology: Model Description and Evaluation. *Journal of Geophysical Research*, 106:73–95, 2001. ISSN 0148-0227. doi: 10.1029/2001JD000807.
- Edwin F. Danielsen. Stratospheric-Tropospheric Exchange Based on Radioactivity, Ozone and Potential Vorticity, 1968. ISSN 0022-4928.
- S S Das, M V Ratnam, K N Uma, K V Subrahmanyam, and I A Girach. Influence of tropical cyclones on tropospheric ozone : possible implication. *Atmospheric Chemistry and Physics (Discussions)*, 15(2003):19305–19323, 2016. ISSN 1680-7324. doi: 10.5194/acpd-15-19305-2015.
- D P Dee, S M Uppala, A J Simmons, P Berrisford, P Poli, S Kobayashi, U Andrae, M A Balmaseda, G Balsamo, P Bauer, P Bechtold, A C M Beljaars, L van de Berg, J Bidlot, N Bormann, C Delsol, R Dragani, M Fuentes, A J Geer, L Haimberger, S B Healy, H Hersbach, E V HÅ³lm, L Isaksen, P KÅ¥llberg, M KÅ¥hler, M Matricardi, A P McNally, B M Monge-Sanz, J.-J. Morcrette, B.-K. Park, C Peubey, P de Rosnay, C Tavolato, J.-N. ThÅ©paut, and F Vitart. The ERA-Interim reanalysis: configuration and performance of the data assimilation system. *Quarterly Journal of the*

- Royal Meteorological Society*, 137(656):553–597, 2011. ISSN 1477-870X. doi: 10.1002/qj.828. URL <http://dx.doi.org/10.1002/qj.828>.
- Sebastian D. Eastham, Debra K. Weisenstein, and Steven R H Barrett. Development and evaluation of the unified tropospheric-stratospheric chemistry extension (UCX) for the global chemistry-transport model GEOS-Chem. *Atmospheric Environment*, 89:52–63, 2014. ISSN 13522310. doi: 10.1016/j.atmosenv.2014.02.001. URL <http://dx.doi.org/10.1016/j.atmosenv.2014.02.001>.
- D. P. Edwards. Tropospheric ozone over the tropical Atlantic: A satellite perspective. *Journal of Geophysical Research*, 108(D8):4237, 2003. ISSN 0148-0227. doi: 10.1029/2002JD002927. URL <http://doi.wiley.com/10.1029/2002JD002927>.
- D. P. Edwards, L. K. Emmons, J. C. Gille, A. Chu, J. L. Attié, L. Giglio, S. W. Wood, Jim Haywood, M. N. Deeter, S. T. Massie, D. C. Ziskin, and James R. Drummond. Satellite-observed pollution from Southern Hemisphere biomass burning. *Journal of Geophysical Research Atmospheres*, 111(14):1–17, 2006. ISSN 01480227. doi: 10.1029/2005JD006655.
- P. Forster, V. Ramaswamy, P. Artaxo, T. Berntsen, R. Betts, D.W. Fahey, J. Haywood, J. Lean, D.C. Lowe, G. Myhre, J. Nganga, R. Prinn, G. Raga, M. Schulz, and R. Van Dorland. Changes in Atmospheric Constituents and in Radiative Forcing. In: *Climate Change 2007: The Physical Science Basis. Contribution of Working Group I to the Fourth Assessment Report of the Intergovernmental Panel on Climate Change*[Solomon, S., D. Qin, M. Man, 2007. URL [https://www.ipcc.ch/publications\\_and\\_data/ar4/wg1/en/ch2.html](https://www.ipcc.ch/publications_and_data/ar4/wg1/en/ch2.html).
- W. Frey, R. Schofield, P. Hoor, D. Kunkel, F. Ravagnani, a. Ulanovsky, S. Viciani, F. D’Amato, and T. P. Lane. The impact of overshooting deep convection on local transport and mixing in the tropical upper troposphere/lower stratosphere (UTLS). *Atmospheric Chemistry and Physics*, 15(11):6467–6486, 2015. ISSN 1680-7324. doi: 10.5194/acp-15-6467-2015. URL <http://www.atmos-chem-phys.net/15/6467/2015/>.
- E. Galani. Observations of stratosphere-to-troposphere transport events over the eastern Mediterranean using a ground-based lidar system. *Journal of Geophysical Research*, 108(D12):1–10, 2003. ISSN 0148-0227. doi: 10.1029/2002JD002596. URL <http://www.agu.org/pubs/crossref/2003/2002JD002596.shtml>.
- Annemieke Gloudemans, Jos De Laat, Maarten Krol, Jan Fokke Meirink, Guido Van Der Werf, Hans Schrijver, and Ilse Aben. Evidence for long-range transport of carbon monoxide in the Southern Hemisphere from SCIAMACHY observations. *European Space Agency, (Special Publication) ESA SP*, 33(SP-636):1–5, 2007. ISSN 03796566. doi: 10.1029/2006GL026804.

- A. B. Guenther, X. Jiang, C. L. Heald, T. Sakulyanontvittaya, T. Duhl, L. K. Emmons, and X. Wang. The model of emissions of gases and aerosols from nature version 2.1 (MEGAN2.1): An extended and updated framework for modeling biogenic emissions. *Geoscientific Model Development*, 5(6):1471–1492, 2012. ISSN 1991959X. doi: 10.5194/gmd-5-1471-2012.
- Ben Henderson. TOMS OH Fix, 2016. URL [http://wiki.seas.harvard.edu/geos-chem/index.php/FAST-JX\\_v7.0\\_photolysis\\_mechanism#Fix\\_for\\_TOMS\\_to\\_address\\_strange\\_cycle\\_in\\_OH\\_output](http://wiki.seas.harvard.edu/geos-chem/index.php/FAST-JX_v7.0_photolysis_mechanism#Fix_for_TOMS_to_address_strange_cycle_in_OH_output).
- M C Jacobson and H Hansson. Organic atmospheric aerosols: Review and state of the science. *Reviews of Geophysics*, (38):267–294, 2000. ISSN 87551209. doi: 10.1029/1998RG000045.
- Daniel a. Jaffe and Nicole L. Wigder. Ozone production from wildfires: A critical review. *Atmospheric Environment*, 51:1–10, 2012. ISSN 13522310. doi: 10.1016/j.atmosenv.2011.11.063. URL <http://dx.doi.org/10.1016/j.atmosenv.2011.11.063>.
- A. O. Langford, J. Brioude, O. R. Cooper, C. J. Senff, R. J. Alvarez, R. M. Hardesty, B. J. Johnson, and S. J. Oltmans. Stratospheric influence on surface ozone in the Los Angeles area during late spring and early summer of 2010. *Journal of Geophysical Research Atmospheres*, 117(3):1–17, 2012. ISSN 01480227. doi: 10.1029/2011JD016766.
- Allen S. Lefohn, Heini Wernli, Douglas Shadwick, Sebastian Limbach, Samuel J. Oltmans, and Melvyn Shapiro. The importance of stratospheric-tropospheric transport in affecting surface ozone concentrations in the western and northern tier of the United States. *Atmospheric Environment*, 45(28):4845–4857, 2011. ISSN 13522310. doi: 10.1016/j.atmosenv.2011.06.014. URL <http://dx.doi.org/10.1016/j.atmosenv.2011.06.014>.
- Meiyun Lin, Arlene M. Fiore, Owen R. Cooper, Larry W. Horowitz, Andrew O. Langford, Hiram Levy, Bryan J. Johnson, Vaishali Naik, Samuel J. Oltmans, and Christoph J. Senff. Springtime high surface ozone events over the western United States: Quantifying the role of stratospheric intrusions. *Journal of Geophysical Research Atmospheres*, 117(19):1–20, 2012. ISSN 01480227. doi: 10.1029/2012JD018151.
- Junhua Liu, Jose M. Rodriguez, Anne M. Thompson, Jennifer A. Logan, Anne R. Douglass, Mark A. Olsen, Stephen D. Steenrod, and Françoise Posny. Origins of tropospheric ozone interannual variation over Réunion: A model investigation. *Journal of Geophysical Research Atmospheres*, pages 1–19, 2015. doi: 10.1002/2015JD023981. URL <http://onlinelibrary.wiley.com/doi/10.1002/2015JD023981/abstract>.
- C H Mari, G Cailley, L Corre, M Saunois, Atti’ E, J L, V Thouret, and A Stohl. Tracing biomass burning plumes from the Southern Hemisphere

- during the AMMA 2006 wet season experiment, *Atmos. Atmospheric Chemistry and Physics*, 8:3951–3961, 2008. ISSN 1680-7324. doi: 10.5194/acpd-7-17339-2007.
- M Mihalikova, S Kirkwood, J Arnault, and D Mikhaylova. Observation of a tropopause fold by MARA VHF wind-profiler radar and ozonesonde at Wasa, Antarctica: comparison with ECMWF analysis and a WRF model simulation. *Annales Geophysicae*, 30(9):1411–1421, 2012. doi: 10.5194/angeo-30-1411-2012. URL <http://www.ann-geophys.net/30/1411/2012/>.
- N. Mze, A. Hauchecorne, H. Bencherif, F. Dalaudier, and J. L. Bertaux. Climatology and comparison of ozone from ENVISAT/GOMOS and SHADOZ/balloon-sonde observations in the southern tropics. *Atmospheric Chemistry and Physics*, 10(16):8025–8035, 2010. ISSN 16807316. doi: 10.5194/acp-10-8025-2010.
- NOAA. NOAA Ozone sondes appendix. URL <http://www.ndsc.ncep.noaa.gov/organize/protocols/appendix5/>.
- Mark a. Olsen. A comparison of Northern and Southern Hemisphere cross-tropopause ozone flux. *Geophysical Research Letters*, 30(7):1412, 2003. ISSN 0094-8276. doi: 10.1029/2002GL016538. URL <http://doi.wiley.com/10.1029/2002GL016538>.
- B.C.a Pak, R.L.b Langenfelds, S.A.b Young, R.J.b Francey, C.P.b Meyer, L.M.b Kivlighon, L.N.b Cooper, B.Lb Dunse, C.E.b Allison, L.P.b Steele, IE.b Galbally, and I.A.b Weeks. Measurements of biomass burning influences in the troposphere over southeast Australia during the SAFARI 2000 dry season campaign. *Journal of Geophysical Research D: Atmospheres*, 108(13):SAF 16–1 – SAF 16–10, 2003. ISSN 0148-0227. doi: 10.1029/2002JD002343. URL <http://www.scopus.com/inward/record.url?eid=2-s2.0-0742322536&partnerID=40&md5=cafaeef03b948fb456696583ed3ab9a5>.
- J. D. Price and G. Vaughan. The potential for stratosphere-troposphere exchange in cut-off-low systems. *Quarterly Journal of the Royal Meteorological Society*, 119(510):343–365, 1993. doi: 10.1002/qj.49711951007. URL <http://onlinelibrary.wiley.com/doi/10.1002/qj.49711951007/abstract>.
- P. Reutter, B. Škerlak, M. Sprenger, and H. Wernli. Stratosphere-troposphere exchange (STE) in the vicinity of North Atlantic cyclones. *Atmospheric Chemistry and Physics*, 15(19):10939–10953, 2015. ISSN 16807324. doi: 10.5194/acp-15-10939-2015.
- N E Selin, S Wu, K M Nam, J M Reilly, S Paltsev, R G Prinn, and M D Webster. Global health and economic impacts of future ozone pollution. *Environmental Research Letters*, 4(4):044014, 2009. ISSN 1748-9326. doi: 10.1088/1748-9326/4/4/044014.

- Parikhith Sinha, Lyatt Jaeglé, Peter V. Hobbs, and Qing Liang. Transport of biomass burning emissions from southern Africa. *Journal of Geophysical Research*, 109:D20204, 2004. ISSN 01480227. doi: 10.1029/2004JD005044.
- Herman G J Smit, Wolfgang Straeter, Bryan J. Johnson, Samuel J. Oltmans, Jonathan Davies, David W. Tarasick, Bruno Hoegger, Rene Stubi, Francis J. Schmidlin, T. Northam, Anne M. Thompson, Jacquelyn C. Witte, Ian Boyd, and Françoise Posny. Assessment of the performance of ECC-ozonesondes under quasi-flight conditions in the environmental simulation chamber: Insights from the Juelich Ozone Sonde Intercomparison Experiment (JOSIE). *Journal of Geophysical Research Atmospheres*, 112(19):1–18, 2007. ISSN 01480227. doi: 10.1029/2006JD007308.
- Michael Sprenger, Mischa Croci Maspoli, and Heini Wernli. Tropopause folds and cross-tropopause exchange: A global investigation based upon ECMWF analyses for the time period March 2000 to February 2001. *Journal of Geophysical Research: Atmospheres*, 108(D12):n/a—n/a, 2003. ISSN 2156-2202. doi: 10.1029/2002JD002587. URL <http://dx.doi.org/10.1029/2002JD002587>.
- D S Stevenson, F J Dentener, M G Schultz, K Ellingsen, T P C van Noije, O Wild, G Zeng, M Amann, C S Atherton, N Bell, D J Bergmann, I Bey, T Butler, J Cofala, W J Collins, R G Derwent, R M Doherty, J Drevet, H J Eskes, A M Fiore, M Gauss, D A Hauglustaine, L W Horowitz, I S A Isaksen, M C Krol, J.-F. Lamarque, M G Lawrence, V Montanaro, J.-F. Müller, G Pitari, M J Prather, J A Pyle, S Rast, J M Rodriguez, M G Sanderson, N H Savage, D T Shindell, S E Strahan, K Sudo, and S Szopa. Multimodel ensemble simulations of present-day and near-future tropospheric ozone. *J. Geophys. Res.*, 111(D8), 2006. doi: 10.1029/2005jd006338. URL <http://dx.doi.org/10.1029/2005JD006338>.
- Andreas Stohl, Heini Wernli, Paul James, Michel Bourqui, Caroline Forster, Mark A. Liniger, Petra Seibert, and Michael Sprenger. A new perspective of stratosphere-troposphere exchange. *Bulletin of the American Meteorological Society*, 84(11):1565–1573+1473, 2003. ISSN 00030007. doi: 10.1175/BAMS-84-11-1565.
- Q. Tang and M. J. Prather. Correlating tropospheric column ozone with tropopause folds: The Aura-OMI satellite data. *Atmospheric Chemistry and Physics*, 10(19):9681–9688, 2010. ISSN 16807316. doi: 10.5194/acp-10-9681-2010.
- Q. Tang and M. J. Prather. Five blind men and an elephant: can NASA Aura measurements quantify the stratosphere-troposphere exchange of ozone flux? *Atmospheric Chemistry and Physics*, 11(5):2357–2380, 2012. ISSN 16807316. doi: 10.5194/acp-12-2357-2012. URL <http://dx.doi.org/10.5194/acpd-11-26897-2011>.

- Yukio Terao, Jennifer A Logan, Anne R Douglass, and Richard S Stolarski. Contribution of stratospheric ozone to the interannual variability of tropospheric ozone in the northern extratropics. *J. Geophys. Res.*, 113(D18), 2008. doi: 10.1029/2008jd009854. URL <http://dx.doi.org/10.1029/2008jd009854>.
- A. M. Thompson, N. V. Balashov, J. C. Witte, J. G R Coetzee, V. Thouret, and F. Posny. Tropospheric ozone increases over the southern Africa region: Bellwether for rapid growth in Southern Hemisphere pollution? *Atmospheric Chemistry and Physics*, 14(18):9855–9869, 2014. ISSN 16807324. doi: 10.5194/acp-14-9855-2014.
- Yoshihiro Tomikawa, Yashiro Nishimura, and Takashi Yamanouchi. Characteristics of Tropopause and Tropopause Inversion Layer in the Polar Region. *SOLA*, 5:141–144, 2009. doi: 10.2151/sola.2009-036. URL <http://dx.doi.org/10.2151/sola.2009-036>.
- G Vaughan, J D Price, and A Howells. Transport into the troposphere in a tropopause fold. *Quarterly Journal of the Royal Meteorological Society*, 120(518):1085–1103, 1993. ISSN 00359009. doi: 10.1002/qj.49712051814.
- Volkmar Wirth. Diabatic heating in an axisymmetric cut-off cyclone and related stratosphere-troposphere exchange. *Quarterly Journal of the Royal Meteorological Society*, 121(521):127–147, 1995. ISSN 00359009. doi: 10.1002/qj.49712152107. URL <http://doi.wiley.com/10.1002/qj.49712152107>.
- World Meteorological Organization WMO. Meteorology A Three-Dimensional Science. *Geneva, Second Session of the Commission for Aerology*, 4:134–138, 1957.
- L Zhang, D J Jacob, X Yue, N V Downey, D A Wood, and D Blewitt. Sources contributing to background surface ozone in the US Intermountain West. *Atmos. Chem. Phys.*, 14(11):5295–5309, 2014. doi: 10.5194/acp-14-5295-2014. URL <http://dx.doi.org/10.5194/acp-14-5295-2014>.